PROCEEDINGS OF SCIENCE

Dineutrino modes probing lepton flavor violation

Rigo Bause,[a] **Hector Gisbert,**[a,*] **Marcel Golz**[a] **and Gudrun Hiller**[a]

[a] *Fakultät für Physik, TU Dortmund, Otto-Hahn-Str. 4, D-44221 Dortmund, Germany*

E-mail: rigo.bause@tu-dortmund.de, hector.gisbert@tu-dortmund.de, marcel.golz@tu-dortmund.de, ghiller@physik.uni-dortmund.de

$SU(2)_L$–invariance links charged dilepton $\bar{q}\, q'\, \ell^+\, \ell^-$ and dineutrino $\bar{q}\, q'\, \bar{\nu}\, \nu$ couplings. This connection can be established using the Standard Model Effective Field Theory framework, and allows to perform complementary experimental tests of lepton universality and charged lepton flavor conservation with flavor-summed dineutrino observables. We present its phenomenological implications for the branching ratios of rare charm decays $c \to u\, \nu\, \bar{\nu}$ and rare B decays $b \to s\, \bar{\nu}\, \nu$ decays.

The European Physical Society Conference on High Energy Physics (EPS-HEP2021), 26-30 July 2021
Online conference, jointly organized by Universität Hamburg and the research center DESY

*Speaker

PoS(EPS-HEP2021)563

1. Introduction

Flavor-changing neutral currents (FCNCs) of q^α and q^β quarks induced by $|\Delta q^\alpha| = |\Delta q^\beta| = 1$ processes represent excellent probes of New Physics (NP) beyond the Standard Model (SM). Their weak loop suppression triggered by the Glashow-Iliopoulos-Maiani (GIM) mechanism and Cabibbo-Kobayashi-Maskawa (CKM) hierarchies, not necessarily present in SM extensions, can result in large experimental deviations from the SM predictions alluding to a breakdown of SM symmetries. In addition, its environment is enriched with further tests if leptons are involved, that is $q_\alpha q_\beta\,\ell_i^+\ell_j^-$ and $q_\alpha q_\beta\,\bar{\nu}_i\nu_j$. We exploit the $SU(2)_L$-link between left-handed charged lepton and neutrino couplings, which may be used to assess charged lepton flavor conservation (cLFC) and lepton universality (LU) quantitatively using flavor-summed dineutrino observables [1]. This link (3) is presented for $|\Delta q^\alpha| = |\Delta q^\beta| = 1$ processes, but we stress that it holds analogously for other conserved quark transitions, both in the up- and down-sector.

These proceedings are organized as follows: In Section 2, we present the effective theory framework where the $SU(2)_L$–link between neutrino and charged lepton couplings is derived. In Sections 3 and 4, we work out its phenomenological implications for charm and beauty, respectively. The conclusions are drawn in Section 5. The results are based on Refs. [1–3], we refer there for further details.

2. $SU(2)_L$–link between dineutrino and charged dilepton couplings

At lowest order in the SM effective field theory (SMEFT), the Lagrangian accounting for semileptonic (axial-)vector four-fermion operators is given by [4],

$$\mathcal{L}_{\rm eff} \supset \frac{C^{(1)}_{\ell q}}{v^2}\bar{Q}\gamma_\mu Q\,\bar{L}\gamma^\mu L + \frac{C^{(3)}_{\ell q}}{v^2}\bar{Q}\gamma_\mu\tau^a Q\,\bar{L}\gamma^\mu\tau^a L + \frac{C_{\ell u}}{v^2}\bar{U}\gamma_\mu U\,\bar{L}\gamma^\mu L + \frac{C_{\ell d}}{v^2}\bar{D}\gamma_\mu D\,\bar{L}\gamma^\mu L\,. \quad (1)$$

Reading off couplings to dineutrinos (C_A^N) and charged dileptons (K_A^N) by writing the operators (1) into $SU(2)_L$-components, one obtains

$$\begin{aligned} C_L^U &= K_L^D = \frac{2\pi}{\alpha}\left(C^{(1)}_{\ell q} + C^{(3)}_{\ell q}\right),\; C_R^U = K_R^U = \frac{2\pi}{\alpha}C_{\ell u}\,,\\ C_L^D &= K_L^U = \frac{2\pi}{\alpha}\left(C^{(1)}_{\ell q} - C^{(3)}_{\ell q}\right),\; C_R^D = K_R^D = \frac{2\pi}{\alpha}C_{\ell d}\,, \end{aligned} \quad (2)$$

where $N = U$ ($N = D$) represents the up-quark sector (down-quark sector), and $A = L(R)$ denotes left- (right-) handed quark currents. Interestingly, $C_R^N = K_R^N$ holds model-independently, while C_L^N is not fixed by K_L^N in general due to the different relative signs of $C^{(1)}_{\ell q}$ and $C^{(3)}_{\ell q}$. Expressing Eqs. (2) in the mass basis, that is $C_L^N = W^\dagger\,\mathcal{K}_L^M\,W + O(\lambda)$, $C_R^N = W^\dagger\,\mathcal{K}_R^N\,W$ where W is the Pontecorvo-Maki-Nakagawa-Sakata (PMNS) matrix and $\lambda \sim 0.2$ the Wolfenstein parameter, and summing lepton flavors i, j incoherently, one obtains the following identity [1]

$$\sum_{\nu=i,j}\left(|C_L^{Nij}|^2 + |C_R^{Nij}|^2\right) = \sum_{\ell=i,j}\left(|\mathcal{K}_L^{Mij}|^2 + |\mathcal{K}_R^{Nij}|^2\right) + O(\lambda)\,, \quad (3)$$

between charged lepton couplings $\mathcal{K}_{L,R}$ and neutrino ones $C_{L,R}$.[1] Here, we use $N, M = U, D$ when the link is exploited for neutrino couplings in the up-quark sector, while $N, M = D, U$ for

[1]Wilson coefficients in calligraphic style denote those for mass eigenstates.

the down-quark sector. Eq. (3) allows the prediction of dineutrino rates for different leptonic flavor structures $\mathcal{K}_{L,R}^{N\,ij}$,

i) $\mathcal{K}_{L,R}^{N\,ij} \propto \delta_{ij}$, *i.e. lepton-universality* (LU),

ii) $\mathcal{K}_{L,R}^{N\,ij}$ diagonal, *i.e. charged lepton flavor conservation* (cLFC),

iii) $\mathcal{K}_{L,R}^{N\,ij}$ arbitrary,

which can be probed with lepton-specific measurements. In the following sections, we use the following notation *i.e.* $\mathcal{K}_{L,R}^{bsij} = \mathcal{K}_{L,R}^{D_{23}ij}$, $C_{L,R}^{bsij} = C_{L,R}^{D_{23}ij}$, etc., to improve the readability.

	ee	$\mu\mu$	$\tau\tau$	$e\mu$	$e\tau$	$\mu\tau$
$R^{\ell\ell'}$	21	6.0	77	6.6	59	70
$\delta R^{\ell\ell'}$	19	5.4	69	5.7	55	63
$r^{\ell\ell'}$	39	11	145	12	115	133

Table 1: Bounds on $|\Delta c| = |\Delta u| = 1$ parameters $R^{\ell\ell'}$ and $\delta R^{\ell\ell'}$ from Eqs. (4), as well as their sum, $r^{\ell\ell'} = R^{\ell\ell'} + \delta R^{\ell\ell'}$. Table taken from Ref. [2].

3. Predictions for charm

In this section, we study the implications of (3) for $c \to u\,\nu\bar{\nu}$ dineutrino transitions, where the situation is exceptional as the SM amplitude is fully negligible due to an efficient GIM-suppression [5] and the current lack of experimental constraints. We use upper limits on $\mathcal{K}_A^{N\,\ell\ell'}$ from high–p_T [6, 7], which allow to set constraints on

$$\begin{aligned} R^{\ell\ell'} &= |\mathcal{K}_L^{sd\ell\ell'}|^2 + |\mathcal{K}_R^{cu\ell\ell'}|^2\,, \qquad R_{\pm}^{\ell\ell'} = |\mathcal{K}_L^{sd\ell\ell'} \pm \mathcal{K}_R^{cu\ell\ell'}|^2, \\ \delta R^{\ell\ell'} &= 2\,\lambda\,\mathrm{Re}\left\{\mathcal{K}_L^{sd\ell\ell'}\mathcal{K}_L^{ss\ell\ell'*} - \mathcal{K}_L^{sd\ell\ell'}\mathcal{K}_L^{dd\ell\ell'*}\right\}, \end{aligned} \tag{4}$$

which directly enter in $c \to u\,\nu\bar{\nu}$ branching ratios. Upper limits on $R^{\ell\ell'}$, $\delta R^{\ell\ell'}$ and their sum $r^{\ell\ell'} = R^{\ell\ell'} + \delta R^{\ell\ell'}$ are provided in Table 1. Since the neutrino flavors are not tagged, the branching ratio is obtained by an incoherent sum

$$\mathcal{B}\left(c \to u\,\nu\bar{\nu}\right) = \sum_{i,j} \mathcal{B}\left(c \to u\,\nu_i\bar{\nu}_j\right) \propto x_{uc}\,, \tag{5}$$

where $x_{uc} = \sum_{i,j}\left(|C_L^{Uij}|^2 + |C_R^{Uij}|^2\right)$. Using (3) with $N, M = U, D$ and Table 1, we obtain upper limits for the different benchmarks *i)-iii)*:

$$x_{uc} = 3\,r^{\mu\mu} \lesssim 34\,, \quad \text{(LU)} \tag{6}$$

$$x_{uc} = r^{ee} + r^{\mu\mu} + r^{\tau\tau} \lesssim 196\,, \quad \text{(cLFC)} \tag{7}$$

$$x_{uc} = r^{ee} + r^{\mu\mu} + r^{\tau\tau} + 2\left(r^{e\mu} + r^{e\tau} + r^{\mu\tau}\right) \lesssim 716\,. \tag{8}$$

Since dimuon bounds are the most stringent ones, see Table 1, they set the LU-limit (6). Experimental measurements above the upper limit in (6) would indicate a breakdown of LU, while values above the limit in (7) would imply a violation of cLFC. Corresponding upper limits on branching ratios of dineutrino modes of a charmed hadron h_c into a final hadronic state F,

$$\mathcal{B}(h_c \to F\,\nu\bar{\nu}) = A_+^{h_c F}\, x_{cu}^+ + A_-^{h_c F}\, x_{cu}^- \,, \tag{9}$$

are provided in Table 2 for several decays modes. The $A_\pm^{h_c F}$ coefficients in Eq. (9) are given in the second column of Table 2. Using the limits (6), (7), (8), together with Eq. (9) and the values of $A_\pm^{h_c F}$, we obtain upper limits on branching ratios for the three flavor scenarios $\mathcal{B}_{\rm LU}^{\rm max}$, $\mathcal{B}_{\rm cLFC}^{\rm max}$, and $\mathcal{B}^{\rm max}$. A branching ratio measurement $\mathcal{B}_{\rm exp}$ within $\mathcal{B}_{\rm LU}^{\rm max} < \mathcal{B}_{\rm exp} < \mathcal{B}_{\rm cLFC}^{\rm max}$ would be a clear signal of LU violation. In contrast, a branching ratio above $\mathcal{B}_{\rm cLFC}^{\rm max}$ would imply a breakdown of cLFC.

$h_c \to F$	$A_+^{h_c F}$ $[10^{-8}]$	$A_-^{h_c F}$ $[10^{-8}]$	$\mathcal{B}_{\rm LU}^{\rm max}$ $[10^{-7}]$	$\mathcal{B}_{\rm cLFC}^{\rm max}$ $[10^{-6}]$	$\mathcal{B}^{\rm max}$ $[10^{-6}]$
$D^0 \to \pi^0$	0.9	–	6.1	3.5	13
$D^+ \to \pi^+$	3.6	–	25	14	52
$D_s^+ \to K^+$	0.7	–	4.6	2.6	9.6
$D^0 \to \pi^0\pi^0$	$\mathcal{O}(10^{-3})$	0.21	1.5	0.8	3.1
$D^0 \to \pi^+\pi^-$	$\mathcal{O}(10^{-3})$	0.41	2.8	1.6	5.9
$D^0 \to K^+K^-$	$\mathcal{O}(10^{-6})$	0.004	0.03	0.02	0.06
$\Lambda_c^+ \to p^+$	1.0	1.7	18	11	39
$\Xi_c^+ \to \Sigma^+$	1.8	3.5	36	21	76
$D^0 \to X$	2.2	2.2	15	8.7	32
$D^+ \to X$	5.6	5.6	38	22	80
$D_s^+ \to X$	2.7	2.7	18	10	38

Table 2: Coefficients $A_\pm^{h_c F}$, as defined in (9), and model-independent upper limits on $\mathcal{B}_{\rm LU}^{\rm max}$, $\mathcal{B}_{\rm cLFC}^{\rm max}$, $\mathcal{B}^{\rm max}$ from (6), (7) and (8), respectively, corresponding to the lepton flavor symmetry benchmarks *i)-iii)*. Table taken from Ref. [2].

4. Testing lepton universality with $b \to s\,\nu\bar{\nu}$

In this section we study $b \to s\,\nu\bar{\nu}$ transitions and their interplay with $b \to s\,\ell^+\ell^-$ transitions routed by (3). The branching ratios for $B \to V\,\nu\bar{\nu}$ and $B \to P\,\nu\bar{\nu}$ decays in the LU limit are given by

$$\mathcal{B}(B \to V\,\nu\bar{\nu})_{\rm LU} = A_+^{BV}\, x_{bs,{\rm LU}}^+ + A_-^{BV}\, x_{bs,{\rm LU}}^- \,, \quad \mathcal{B}(B \to P\,\nu\bar{\nu})_{\rm LU} = A_+^{BP}\, x_{bs,{\rm LU}}^+ \,, \tag{10}$$

where $x_{bs,{\rm LU}}^\pm = 3\,\left|C_{\rm SM}^{bs\ell\ell} + \mathcal{K}_L^{tc\ell\ell} \pm \mathcal{K}_R^{bs\ell\ell}\right|^2$, and the values of $A_\pm^{BV}$ and A_+^{BP} for different modes can be found in Ref. [3]. We obtain two solutions for the coupling $\mathcal{K}_L^{tc\ell\ell}$ when we solve $\mathcal{B}(B \to P\,\nu\bar{\nu})_{\rm LU}$ in Eq. (10). Plugging them into Eq. (10) results in a correlation between both LU branching ratios [3]

$$\mathcal{B}(B \to V\,\nu\bar{\nu})_{\rm LU} = \frac{A_+^{BV}}{A_+^{BP}}\,\mathcal{B}(B \to P\,\nu\bar{\nu})_{\rm LU} + 3\,A_-^{BV}\left|\sqrt{\frac{\mathcal{B}(B \to P\,\nu\bar{\nu})_{\rm LU}}{3\,A_+^{BP}}} \mp 2\,\mathcal{K}_R^{bs\ell\ell}\right|^2 . \tag{11}$$

PoS(EPS-HEP2021)563

The most stringent limits on $\mathcal{K}_R^{bs\ell\ell}$ are given for $\ell\ell = \mu\mu$. Performing a 6D global fit of the semileptonic Wilson coefficients $C^{(\prime)}_{(7,9,10),\mu}$ to the current experimental data on $b \to s\,\mu^+\mu^-$ data (excluding $R_{K^{(*)}}$ which can be polluted by NP effects in electron couplings), we obtain the following 1σ fit value [3]

$$\mathcal{K}_R^{bs\ell\ell} = V_{tb}V_{ts}^* \,(0.46 \pm 0.26)\,. \tag{12}$$

Fig. 1 displays the correlation between $\mathcal{B}(B^0 \to K^{*0}\nu\bar{\nu})$ and $\mathcal{B}(B^0 \to K^0\nu\bar{\nu})$, cf. Eq. (11). The SM predictions $\mathcal{B}(B^0 \to K^{*0}\nu\bar{\nu})_{\mathrm{SM}} = (8.2 \pm 1.0)\cdot 10^{-6}$, $\mathcal{B}(B^0 \to K^0\nu\bar{\nu})_{\mathrm{SM}} = (3.9 \pm 0.5)\cdot 10^{-6}$ [3] are depicted as a blue diamond with their $1\,\sigma$ uncertainties (blue bars). We have scanned $\mathcal{K}_R^{bs\mu\mu}$, $A_{\pm}^{B^0K^{*0}}$, and $A_{+}^{B^0K^0}$ within their $1\,\sigma$ $(2\,\sigma)$ regions in Eq. (10), resulting in the dark red region (dashed red lines) which represents the LU region, numerically [3]

$$\frac{\mathcal{B}(B^0 \to K^{*0}\nu\bar{\nu})}{\mathcal{B}(B^0 \to K^0\nu\bar{\nu})} = 1.7\ldots 2.6 \quad (1.3\ldots 2.9)\,. \tag{13}$$

Interestingly, a branching ratio measurement outside the red region would clearly signal evidence for LU violation, but if a future measurement is instead inside this region, this may not necessarily imply LU conservation. Outside the light green region the validity of our effective field theory (EFT) framework gets broken [3]. More stringent limits for specific LU SM extensions are depicted as benchmarks, resulting in best fit values (markers) and $1\,\sigma$ regions (ellipses) for Z' (red star), LQ representations S_3 (pink pentagon) and V_3 (celeste triangle) from $b \to s\,\mu^+\mu^-$ global fits, see Ref. [3] for details. The current experimental 90 % CL upper limits, $\mathcal{B}(B^0 \to K^{*0}\nu\bar{\nu})_{\mathrm{exp}} < 1.8\cdot 10^{-5}$ [8] and $\mathcal{B}(B^0 \to K^0\nu\bar{\nu})_{\mathrm{exp}} < 2.6\cdot 10^{-5}$ [8], are displayed by hatched bands. The gray bands represent the derived EFT limits, $\mathcal{B}(B^0 \to K^0\nu\bar{\nu})_{\mathrm{derived}} < 1.5\cdot 10^{-5}$, from Ref. [3]. A measurement between gray and hatched area would infer a clear hint of NP not covered by our EFT framework, *i.e. light particles*. The projected experimental sensitivity (10 % at the chosen point) of Belle II with 50 ab^{-1} is illustrated by the yellow boxes [9]. Similar conclusions can be drawn in $b \to d\,\nu\bar{\nu}$ decay [3].

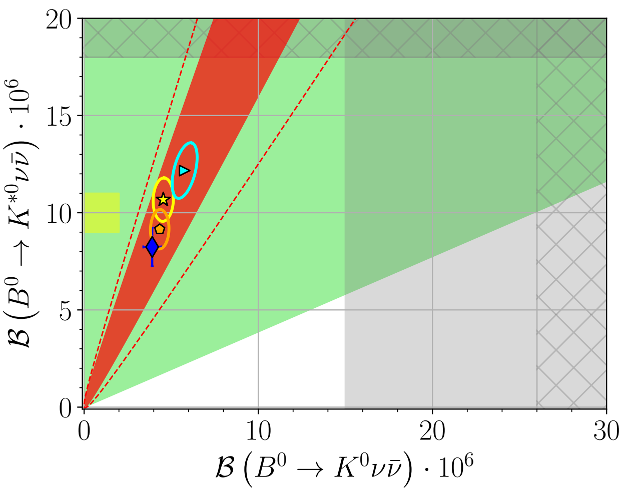

Figure 1: Correlation between $\mathcal{B}(B^0 \to K^{*0}\nu\bar{\nu})$ and $\mathcal{B}(B^0 \to K^0\nu\bar{\nu})$. Details are given in the main text. Figure taken from Ref. [3].

PoS(EPS-HEP2021)563

5. Conclusions

$SU(2)_L$-invariance relates dineutrinos $\bar{q}\, q'\, \bar{\nu}\, \nu$ and charged dilepton couplings $\bar{q}\, q'\, \ell^+\, \ell^-$ in a model-independent way. This link (3) allows probing lepton flavor structure in dineutrino observables in three benchmarks: lepton universality, charged lepton flavor conservation and lepton flavor violation. The link has been exploited for the rare charm and B decays, resulting in novel tests of the aforementioned symmetries, see Table 2 and Eq. (13), respectively. Our predictions are well-suited for the experiments Belle II [9], BES III [10], and future e^+e^--colliders, such as an FCC-ee running at the Z [11], and could offer some insight on the persistent anomalies in B decays.

Acknowlegments

We want to thank the organizers for their effort to make this conference such a successful event. This work is supported by the *Studienstiftung des Deutschen Volkes* (MG) and the *Bundesministerium für Bildung und Forschung* – BMBF (HG).

References

[1] R. Bause, H. Gisbert, M. Golz and G. Hiller, [arXiv:2007.05001 [hep-ph]].

[2] R. Bause, H. Gisbert, M. Golz and G. Hiller, Phys. Rev. D **103** (2021) no.1, 015033 [arXiv:2010.02225 [hep-ph]].

[3] R. Bause, H. Gisbert, M. Golz and G. Hiller, [arXiv:2109.01675 [hep-ph]].

[4] B. Grzadkowski, M. Iskrzynski, M. Misiak and J. Rosiek, JHEP **10** (2010), 085 [arXiv:1008.4884 [hep-ph]].

[5] G. Burdman, E. Golowich, J. L. Hewett and S. Pakvasa, Phys. Rev. D **66**, 014009 (2002) [hep-ph/0112235].

[6] J. Fuentes-Martin, A. Greljo, J. Martin Camalich and J. D. Ruiz-Alvarez, JHEP **11** (2020), 080. [arXiv:2003.12421 [hep-ph]].

[7] A. Angelescu, D. A. Faroughy and O. Sumensari, Eur. Phys. J. C **80**, no.7, 641 (2020) [arXiv:2002.05684 [hep-ph]].

[8] P.A. Zyla *et al.* [Particle Data Group], PTEP **2020**, no.8, 083C01 (2020)

[9] E. Kou *et al.* [Belle-II Collaboration], PTEP **2019**, no. 12, 123C01 (2019) [arXiv:1808.10567 [hep-ex]].

[10] M. Ablikim *et al.*, Chin. Phys. C **44** (2020) no.4, 040001 [arXiv:1912.05983 [hep-ex]].

[11] A. Abada *et al.* [FCC Collaboration], Eur. Phys. J. C **79**, no. 6, 474 (2019).

PoS(EPS-HEP2021)563